Available online at www.sciencedirect.com
SCIENCE DIRECT®
ELSEVIER
Nuclear Instruments and Methods in Physics Research B 202 (2003) 261–268
NIM B
Beam Interactions with Materials & Atoms
www.elsevier.com/locate/nimb

Computer modeling and electron microscopy of silicon surfaces irradiated by cluster ion impacts

Z. Insepov [a,*], L.P. Allen [b], C. Santeufemio [b], K.S. Jones [c], I. Yamada [a]

[a] *Lab. of Adv. Sci. Technol. for Industry, Himeji Institute of Technology, 3-1-2 Kouto, Kamigori, Ako, Hyogo 678-1205, Japan*
[b] *Epion Corporation, 37 Manning Road, Billerica, Massachusetts 01821, USA*
[c] *Department of Materials Science and Engineering, University of Florida, Gainesville, Florida 32611, USA*

Abstract

A hybrid molecular dynamics model has been applied for modeling impacts of Ar and decaborane clusters, with energies ranging from 25 to 1500 eV/atom, impacting Si surfaces. Crater formation, sputtering, and the shapes of craters and rims were studied. Our simulation predicts that on a Si(1 0 0), craters are nearly triangular in cross-section, with the facets directed along the close-packed (1 1 1) planes. The Si(1 0 0) craters exhibit four fold symmetry. The craters on Si(1 1 1) surface are well rounded in cross-section and the top-view shows a complicated six fold or triangular image. The simulation results for individual gas cluster impacts were compared with experiments at low dose (10^{10} ions/cm^2 charge fluence) for Ar impacts into Si(1 0 0) and Si(1 1 1) substrate surfaces. Atomic force microscopy and cross-sectional high-resolution transmission electron microscope imaging of individual gas cluster ion impacts into Si(1 0 0) and Si(1 1 1) substrate surfaces revealed faceting properties of the craters and are in agreement with the theoretical prediction. The sputtering yield from Si(1 0 0) surfaces bombarded with B_{10} cluster ions, with total energy of 1–15 keV, was also calculated. The results of this study will be helpful for the research and development of a new low-damage gas cluster ion beam process technology.

PACS: 02.70.Ns; 61.43.Bn; 34.50.Dy; 61.72.Ff
Keywords: Molecular dynamics; Cluster; Crater; Faceting; AFM; TEM; Implantation

1. Introduction

Interactions of energetic clusters of atoms with solid surfaces demonstrate unique phenomena and promise new applications for surface modification technology [1–6]. Clusters of gaseous elements and compounds consisting of hundreds to thousands of atoms, with energies from a few eV to a few hundreds of eV per cluster atom are of particular interest for surface modification like etching or smoothing.

The main surface modification phenomenon is the surface smoothing effect. A crystal surface, with an initial average surface roughness of tens or hundreds of angstroms, becomes atomically flat, with the residual roughness of about a few angstroms [7–13]. The gas cluster ion beam smoothing typically occurs after irradiation by an ionized Ar_n

* Corresponding author. Tel.: +81-791-58-0412; fax: +81-791-58-0242.
E-mail address: insepov@lasti.himeji-tech.ac.jp (Z. Insepov).

0168-583X/02/$ - see front matter
doi:10.1016/S0168-583X(02)01867-0

($n \sim 1000$–$10{,}000$) cluster beam at the dose of 10^{14}–10^{16} ions/cm^2 fluence. An individual cluster impact would leave a crater on the surface, but it is impossible to experimentally study those craters at high cluster ion doses that are typical for the surface smoothing effect. Therefore, the study of single crater formation, crater structure, and faceting properties are important tasks for understanding the fundamental surface science and are of interest for the surface smoothing effect. While experimental data are still sparse [1,2,4], modeling may help to evaluate these prospects and shed light on the mechanisms involved.

Decaborane cluster ion ($B_{10}H_{14}$) implantation is of a high interest for the silicon industry because this novel technique is being considered as an alternative method for fabricating very shallow p–n junction for future devices [11,12,14]. There is still a lack of information on decaborane bombardment and it is uncertain if it would sputter or smooth silicon surfaces.

The aim of this work is to simulate individual Ar gas and decaborane cluster impacts by molecular dynamics (MD) and compare the calculated cross-sections and faceting properties of the craters with those observed by high-resolution transmission electron microscopy (HRTEM) and atomic force microscopy (AFM). High and low energy Ar and O_2 gas cluster impacts are observed in cross-section by HRTEM. AFM is used to examine the crater surface shapes for the high-energy Ar cluster impacts for two different silicon surface orientations.

2. Molecular dynamics simulation

In MD simulation, the equations of motion of interacting particles are solved numerically. Appropriate initial and boundary conditions are supplied. Due to limited computing resources, there is always a problem of choosing a correct size for the model system.

Energetic cluster impacts create intense collisions between atoms in the central zone where equivalent temperature and pressure may reach 10^5 K and 10^6 bars, respectively [5]. The problem of the boundary conditions for this case can be examined by considering shock waves created by the energetic cluster impact. Unphysical reflections

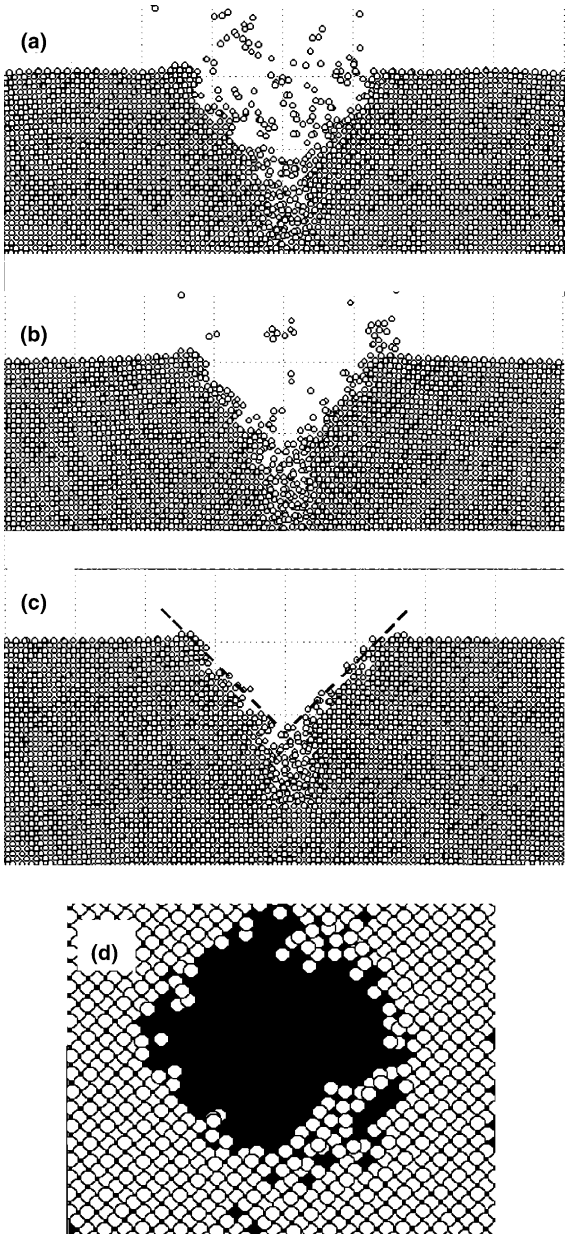

Fig. 1. (a) MD result for the three time instants for side-views of the crater formed by a 25 eV/atom Ar_{369} cluster impact on a Si(1 0 0) surface after time intervals: (a) 2.9, (b) 5.8 and (c) 14.4 ps from the start of cluster collision with the target; d) top-view of the crater formed by a Ar_{135}, 25 eV/atom, cluster impact on a Si(1 0 0) surface.

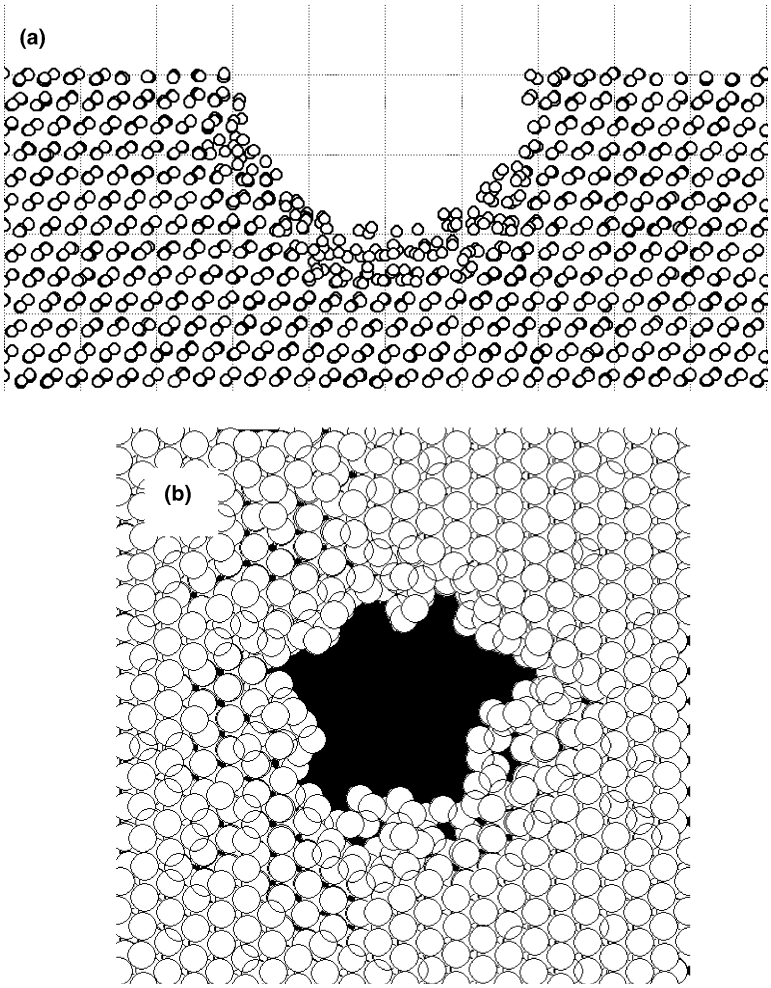

Fig. 2. (a) MD result for the side-view of a crater formed on a Si(1 1 1) surface by a Ar_{135} cluster impact, with energy of 25 eV/atom, 14.4 ps after the beginning of impact. (b) Top-view of the crater formed on a Si(1 1 1) surface by an Ar_{135}, 25 eV/atom, cluster impact. The complicated faceting feature is clearly seen and may be compared with the AFM image of Fig. 4.

of the shock waves from the system boundary may show up in MD results, distorting the picture of the investigated process. Shock wave reflections have been revealed for the systems as large as 4×10^5 target atoms studied by MD if fixed PBC boundaries are used, for the cluster impact energy as low as 10 kV [15,16].

A hybrid model utilizing MD for the atoms in the central collision zone, and continuum mechanics and thermodynamics outside have been used in this study to stabilize the system temperature. The details of the used method could be found elsewhere [17,18]. This hybrid model successfully solves the problem related to a finite system size by reducing the number of the required degrees of freedom, and will be applied to the modeling of crater formation and to calculate sputtering yield in this paper.

In the MD calculations, we used the Buckingham potential [19] to represent two-body forces between cluster atoms and between the cluster and target atoms while interaction between Si atoms were represented by the Stillinger–Weber potential. The cluster was modeled by cutting a spherical

volume from an FCC argon lattice with initial temperature set to zero.

The clusters used in simulations contained about 135–369 atoms and had kinetic energy of 25–100 eV/atom. The cylindrical target model contained $\sim 3 \times 10^5$ atoms in the central MD zone while the continuum mechanics calculations extended to 10 times larger volume.

Implantation of decaborane ions, in the energy range of 1–15 keV, into Si and sputtering of the target was simulated. The decaborane molecule was modeled as a B_{10} cluster. Based on the cluster energy and ion fluence, 10^{13}–10^{16} ion/cm^2, a target consisting of about 2×10^5 Si atoms was used.

The ZBL potential at short distances combined with the Stillinger–Weber potential at equilibrium distances was used to evaluate interactions between two and three Si atoms, as usual [6]. Interaction between B and Si atoms was modeled via the ZBL screened Coulomb potential at short distances, $r < 0.52$ Å, and with a Morse-type potential at long distances, $r > 0.86$ Å. Interaction between two B dopants was modeled with an (exp-6)-type potential, with the depth of 0.2 eV and the equilibrium distance of 1.5 Å.

Silicon atoms were considered as sputtered if they cross a plane $2R_{\text{cut}}$ above the surface and have positive normal velocity component. Sputtering yield was calculated for impacts of 10 clusters with different orientations around the mass center and the result was averaged.

Fig. 1 shows three time instants for side-views of the crater formed by a 25 eV/atom Ar_{369} cluster impact on a Si(1 0 0) surface after time intervals of (a) 2.9, (b) 5.8 and (c) 14.4 ps from the start of cluster collision with the target. This picture shows a nearly triangular faceting of the crater, which is due to a higher energy of the (1 1 1) plane. The top-view of the crater is given in Fig. 1(b). It shows a nearly four fold symmetry crater with facets formed by four (1 1 1) planes crossing the (1 0 0) surface. This figure shows a thin slice of the substrate parallel to surface that was made by cutting out the atoms with the positions within the interval: -3 Å $< zi < 0.05$ Å (three atomic layers from the top of non-irradiated surface).

The Si(1 1 1) surface shows faceting features quite different from that of (1 0 0) surface as can be viewed in Fig. 2(a, b). We see that the side-view (Fig. 2(a)) has a round-shaped crater and the top-view has a six-point shape, previously unobserved in simulation or in experiment. Four atomic layers from the top of non-irradiated surface are shown: -4 Å $< zi < 0.05$ Å.

Fig. 3 presents the result of this simulation for the energy dependence of the total sputtering yield of Si(1 0 0) surface bombarded with B_{10} cluster ions at different energies in the 1–15 keV range. The experimental value of the sputtering yield, 4.0 ± 0.6 sputtered Si atoms at 12 keV per decaborane cluster ion implantation [14]. For energies above 10 keV, the MD data points and the experimental data point could be fitted with an empirical formula $Y = A \exp[-B/(E + C)]$ that was suggested for low-energy sputtering yield from metals bombarded with single ions [20]. The number of reflected boron atoms is also of a keen interest for the future implantation technique. Our calculations show that about 70% of the boron atoms are reflected back into vacuum for energies lower than 1.5 keV, and the reflection probability

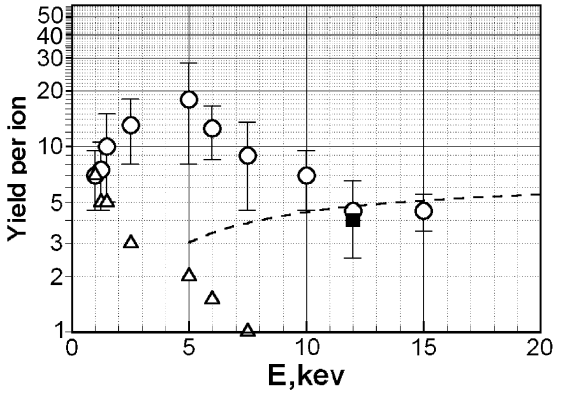

Fig. 3. Si sputtering yield caused by B_{10} cluster implantations, with energies of 1–15 keV, calculated in this paper (circles). The error bars were obtained for the simulations with different B_{10} cluster orientations, relative to the Si(1 0 0) surface. The experimental data point (square) was obtained for a 12 keV implantation of a decaborane ($B_{10}H_{14}$) cluster ion into a thin Si film deposited on a carbon substrate. The dash line shows an empirical relation obtained for low energy sputtering yield of metals: $Y \sim A \exp[-B/(E + C)]$ [20] caused by single ions bombardment. The following parameters: $A = 7$, $B = 5$, $C = 1$ were used for fitting. Triangles show the number of reflected boron atoms.

drops down rapidly for the energies above 5 keV. All boron atoms were implanted at energies higher than about 7.5 keV.

3. Experimental imaging of crater impacts

In this study, polished Si substrates with a native oxide were exposed to a low, 10^{10} ions/cm^2, argon and O_2 gas cluster ions using both 24 and 3 kV acceleration energies. HRTEM cross-section images and AFM imaging of the individual 24 kV Ar cluster impacts were analyzed.

The images of individual gas cluster ion impacts were obtained using a JEOL 2010 TEM with a field-emission gun. Images were formed by orientation of the sample such that the transmitted beam was parallel to the $\langle 1\,1\,0\rangle$ direction of the lattice (i.e. parallel to the (1 0 0) plane of the surface). Fig. 4(a) shows HRTEM cross-section of an individual Ar gas cluster ion crater formed by a 24 kV acceleration into Si(1 0 0). The image cross-section shape agrees well with Fig. 1(a)–(c), showing a conical impact crater with the (1 1 1) planes aligned with the crater walls. Fig. 4(b) shows HRTEM cross-section of a 3 kV individual Ar gas cluster ion crater into a Si(1 0 0) surface. The shape and atomic plane cross-section boundaries appear identical to that of the 24 kV impact crater, but with a much shallower depth of impact.

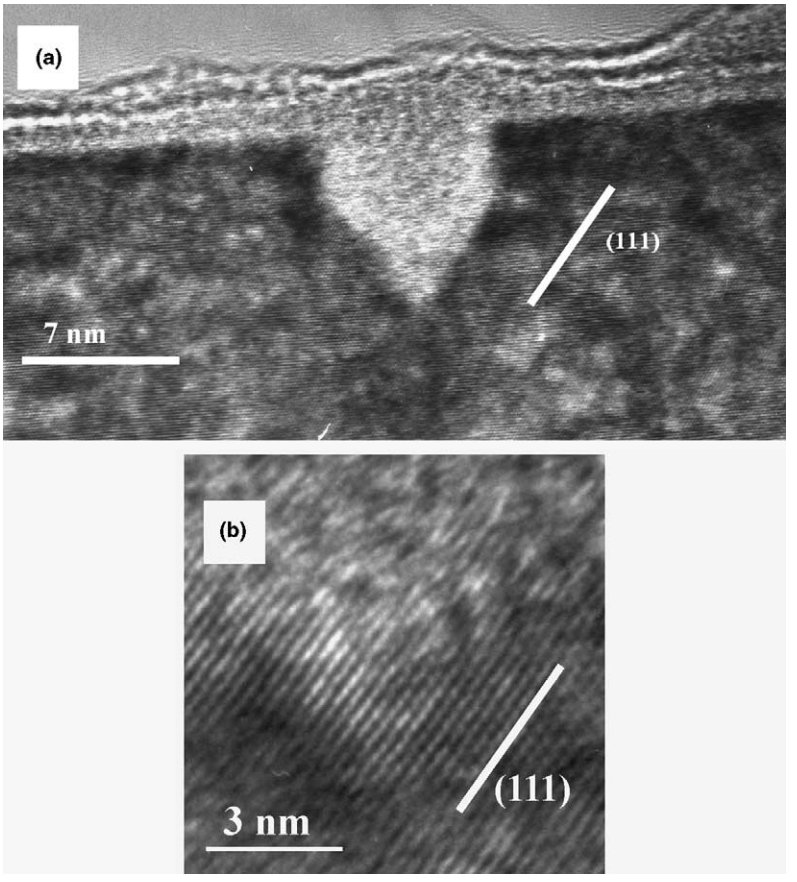

Fig. 4. (a) HRTEM cross-section image of an individual 24 kV Ar gas cluster ion impact into Si(1 0 0). Crater conical edges align along the (1 1 1) lattice planes; (b) HRTEM cross-section image of an individual 3 kV Ar gas cluster ion impact into Si(1 0 0). Crater conical edges align along the (1 1 1) lattice planes, but the depth of impact is reduced.

The 24 and 3 kV individual impact crater images of an O_2 cluster into Si(1 1 1) are shown in Fig. 5(a) and (b), respectively. Once again, the general shape of the impact crater is maintained in the higher and lower energy processes, with the lower energy impact having a shallower crater depth. Within our observation framework, both the O_2 gas cluster impacts of either energy typically result in a more rounded crater shape as compared with that of the Ar impact crater.

The surface of the low fluence GCIB processed Si was imaged by AFM. Fig. 6 shows the surface view of individual hillocks as observed by 100 nm^2 AFM scanned images. The resolution of the AFM tip used is not sufficient to "see" within the crater itself. Fig. 6(a) shows the four fold hillock symmetry formed over a 24 kV Ar gas cluster impact site which reflects the atomic density the Si(1 0 0) substrate. Fig. 6(b) shows the three fold symmetry of the hillocks formed by a 24 kV Ar gas cluster impact into the Si(1 1 1) surface. A continuum of individual hillock heights and diameters has been observed, ranging from just over surface oxide height (~2 nm) to over 5 nm high.

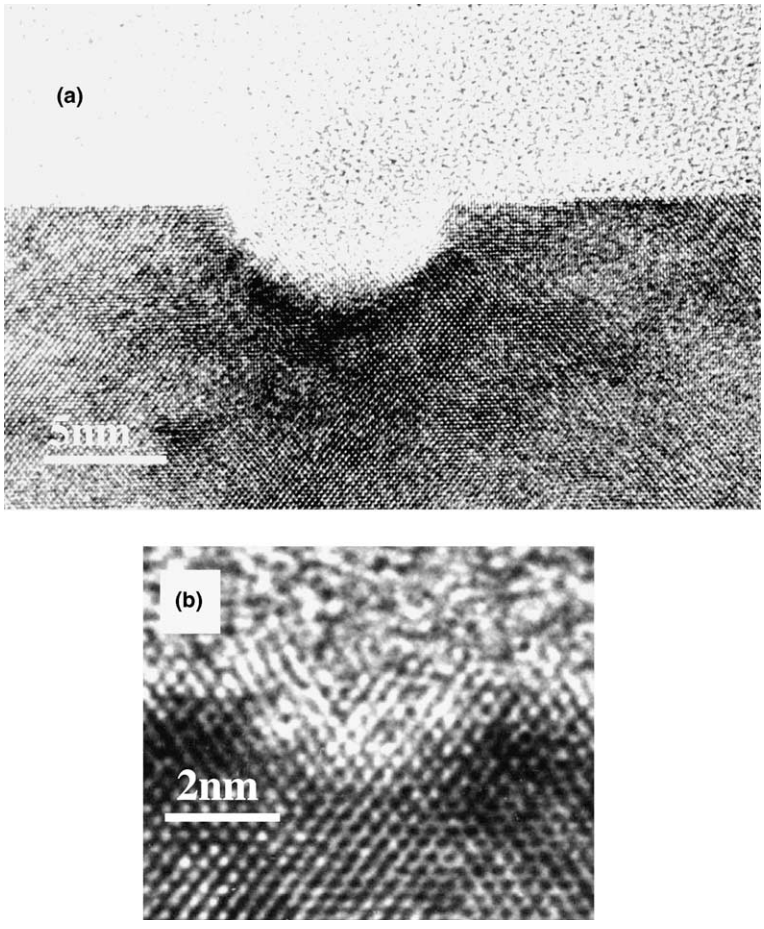

Fig. 5. (a) HRTEM cross-section image of an individual 24 kV O_2 gas cluster ion impact into Si(1 1 1). Rounder impact craters typically resulted from the O_2 cluster process, perhaps from the immediate oxidation of the Si and the change in associated bond strength of the forming crater wall; (b) HRTEM cross-section of an individual 3 kV O_2 gas cluster impact into Si(1 1 1). The rounder shape of the impact is preserved with the shallow depth of the crater.

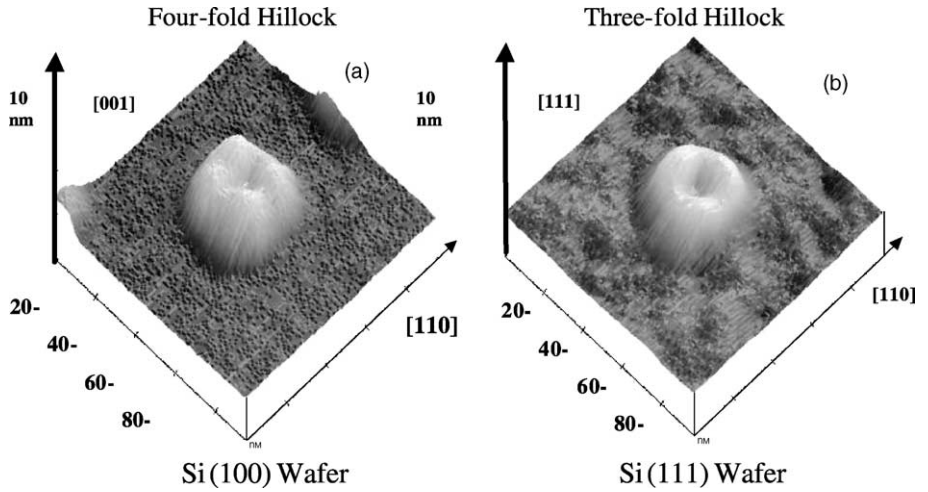

Fig. 6. Three-dimensional AFM image of four fold symmetry of Si(1 0 0) 24 kV Ar cluster impact hillock (a) and three fold symmetry of Si(1 1 1) 24 kV Ar cluster impact hillock (b). Dimensions of both AFM images are 100 nm × 100 nm with a 10 nm height scaling.

4. Conclusion

Further insight on the nature of single gas cluster impacts into a Si surface has been provided. AFM and MD simulation of the craters and hillocks show and predict a four fold symmetry for the 24 kV Ar GCIB individual impacts into Si(1 0 0) and a three fold (six fold) symmetry for the 24 kV Ar GCIB individual impacts into Si(1 1 1). This is consistent with the density of atoms for the respective Si crystal orientations. The effective use of GCIB energy and chemistry for tailoring the smoothing and etching of material surfaces may be explained through the stochastic overlay of the crater depth, crater contour, and individual hillocks to form the finished GCIB processed surface.

The simulation of decaborane implantation has revealed a surprising result that the sputtering yield decreases with increasing the implantation energy, as compared with a single ion implantation. At low energy of 1–1.5 keV, most of boron atoms were reflected back into vacuum. More experiments should be done to confirm these findings.

Acknowledgements

The authors gratefully acknowledge valuable discussions with John Hautala, Tom Tetreault, Yan Shao, Mike Mack and Allen Kirkpatrick of Epion Corporation. This work was partially supported by the NEDO project (Japan). The integral support of the USAF under contract #F33615–00–C–5404 is sincerely acknowledged. GCIB equipment and process work under DoC-NIST ATP award contract #70NANB8H4011 is also appreciated.

References

[1] J.-H. Song, S.N. Kwon, D.-K. Choi, W.-K. Choi, Nucl. Instr. and Meth. B 179 (2001) 568.
[2] L.P. Allen, K.S. Jones, C. Santeufemio, W. Brooks, D.B. Fenner, J. Hautala, in: Proceedings of the Near Surface Effects Conference, 5–10 August 2001, Kodiak Island, Alaska (woodc@onr.navy.mil), Office of Naval Research, Arlington, VA, p. 16.
[3] P. von Blanckenhagen, A. Gruber, J. Gspann, Nucl. Instr. and Meth. B 122 (1997) 322.
[4] A. Gruber, J. Gspann, J. Vac. Sci. Technol. B 15 (6) (1997) 2362.
[5] I. Yamada, J. Matsuo, Z. Insepov, D. Takeuchi, M. Akizuki, N. Toyoda, J. Vac. Sci. Technol. A 14 (1996) 781.
[6] H. Hsieh, R.S. Averback, H. Sellers, C.P. Flynn, Phys. Rev. B 45 (1992) 4417.
[7] Z. Insepov, I. Yamada, Mat. Sci. Eng. A 217–218 (1996) 89.
[8] D.B. Fenner, D.W. Dean, V. DiFilippo, L.P. Allen, J. Hautala, P.B. Mirkarimi, in: S.C. Moss, K.-H. Heinig, D.B. Poker (Eds.), Mat. Res. Soc. Symp. Proc., Vol. 647, Materials Research Society, 2001, p. O5.2.1.
[9] D.B. Fenner, R.P. Torti, L.P. Allen, N. Toyoda, A.R. Kirkpatrick, J.A. Greer, V. DiFilippo, J. Hautala, Mat. Res. Soc. Symp. Proc. 585 (2000) 27.

[10] Z. Insepov, M. Sosnowski, I. Yamada, Adv. Mater.'93, IV/ Laser beam modification of materials, in: I. Yamada et al. (Eds.), Trans. Mat. Res. Soc. Jpn., Vol. 17, 1994, p. 111.
[11] I. Yamada, J. Matsuo, Mat. Res. Soc. Symp. Proc. 396 (1996) 149.
[12] I. Yamada, J. Matsuo, in: K.N. Tu, J.W. Mayer, J.M. Poate, L.L. Chen (Eds.), Mat. Res. Soc., Symp. Proc., Vol. 427, p. 265.
[13] D.B. Fenner, J. Hautala, L.P. Allen, T.G. Tetrault, A. Al-Jibouri, J.I. Budnick, K.S. Jones, J. Vac. Sci. Technol. A 19 (4) (2001) 1207.
[14] M. Sosnowski et al., Appl. Phys. Lett. 80 (2002) 592.
[15] Z. Insepov, I. Yamada, Nucl. Instr. and Meth. B 99 (1995) 248.
[16] M. Moseler, J. Nordiek, H. Haberland, Phys. Rev. B 56 (1997) 15439.
[17] Z. Insepov, M. Sosnowski, I. Yamada, Nucl. Instr. and Meth. B 127–128 (1997) 269.
[18] Z. Insepov, R. Manory, J. Matsuo, I. Yamada, Phys. Rev. B 61 (2000) 8744.
[19] R. Smith, M. Shaw, R.P. Webb, M.A. Foad, J. Appl. Phys. 83 (1998) 3148.
[20] T.G. Eck, L. Chen, J. Appl. Phys., in press.